Liquid Crystals
Publication details, including instructions for authors and subscription information:
http://www.informaworld.com/smpp/title~content=t713926090

Pretilt angle measurements on smectic A cells with chevron and tilted bookshelf layer structures

J. J. Bonvent[ab]; J. A. M. M. Van Haaren[a]; G. Cnossen[a]; A. G. H. Verhulst[a]; P. Van Der Sluis[a]
[a] Philips Research Laboratories, Prof. Holstlaan 4, Eindhoven, The Netherlands [b] Università degli Studi della Calabria, Dipartimento di Fisica, Arcavacata di Rende (CS), Italy

To cite this Article Bonvent, J. J. , Van Haaren, J. A. M. M. , Cnossen, G. , Verhulst, A. G. H. and Van Der Sluis, P.(1995) 'Pretilt angle measurements on smectic A cells with chevron and tilted bookshelf layer structures', Liquid Crystals, 18: 5, 723 — 731
To link to this Article: DOI: 10.1080/02678299508036682
URL: http://dx.doi.org/10.1080/02678299508036682

LIQUID CRYSTALS, 1995, VOL. 18, NO. 5, 723–731

Pretilt angle measurements on smectic A cells with chevron and tilted bookshelf layer structures

by J. J. BONVENT†, J. A. M. M. VAN HAAREN*, G. CNOSSEN, A. G. H. VERHULST and P. VAN DER SLUIS

Philips Research Laboratories, Prof. Holstlaan 4, 5656 AA Eindhoven, The Netherlands

(*Received 21 March 1994; in final form 14 July 1994; accepted 15 August 1994*)

We have measured the pretilt angle induced by rubbed polymer films in a smectic A and in a nematic liquid crystalline medium using an optical phase retardation method. The pretilt angle was found to depend on the liquid crystalline phase (smectic A versus nematic) and on the smectic layer structure (chevron versus tilted-bookshelf). The occurrence of the different smectic layer structures was verified by X-ray diffraction measurements. The effect of the applied rubbing energy on the pretilt angle obtained is measured.

1. Introduction

Rubbing of polymer layers to induce liquid crystal alignment is a standard technique in liquid crystal display technology. In the nematic phase, the liquid crystal molecules are aligned parallel to the rubbing direction, while making a certain angle with the orienting surface (pretilt angle). A non-zero pretilt angle is essential for proper electro-optical performance of many types of displays. The pretilt angle affects, amongst other factors, the transmission-voltage curve [1], the occurrence of reverse-tilt domains [2], the presence of zigzag defects in ferroelectric liquid crystal displays [3] and the multiplex ratio of supertwisted nematic displays [4]. Measurements of the pretilt angle are therefore of practical interest [5, 6]. Generally, these measurements are performed on a homogeneously aligned nematic liquid crystal, because it is then easy to obtain a uniformly aligned sample (see figure 1). Some authors [7] assumed that the pretilt angle in the smectic phases (smectic A or chiral smectic C) is equal to the pretilt angle induced in a nematic liquid crystalline material, aligned with the same and identically rubbed polymer layer. Others have reported a dependence on the liquid crystal phase [8]. Different mechanisms for the generation of a pretilt angle have been proposed: steric, polar, and (dispersive) van der Waals interactions between the rubbed polymer surface and the liquid crystal molecules [9]. In general, the pretilt angle depends on the molecular structure of the orienting polymer, the molecular structure of the liquid crystal and on the liquid crystalline phase (nematic or smectic). To obtain a better understanding of the effect of the smectic layer structure on the pretilt angle, it is necessary to determine the pretilt angle directly in the smectic phase.

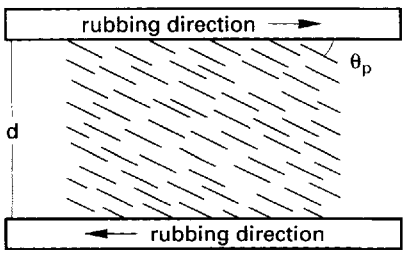

Figure 1. Nematic liquid crystalline material aligned in a cell whose two orienting surfaces have been rubbed in antiparallel directions. The cell thickness d and the pretilt angle θ_p are indicated.

In this paper we present the results of pretilt angle measurements performed on the smectic A phase using an optical-phase retardation method [10]. Two different cell configurations were used to align a smectic A material: parallel and antiparallel rubbing directions of the two aligning surfaces. As known from the literature [11–14], the antiparallel configuration leads to a tilted-bookshelf layer structure (see figure 2), whereas the parallel configuration leads to a chevron layer structure (see figure 3). We verified this for our smectic A material by means of X-ray diffraction experiments. Analytical descriptions of the functional form of the phase retardation are presented for both smectic layer structures. These descriptions are used to derive the pretilt angle from the experimental data by means of a fitting procedure. The

† Present address: Università degli Studi della Calabria, Dipartimento di Fisica, 87036 Arcavacata di Rende (CS), Italy.
* Author for correspondence.

0267–8292/95 $10·00

effects of the applied rubbing strength on the pretilt angles obtained for the two different smectic layer structures and for the nematic phase are compared.

2. Experimental

2.1. *Liquid crystal cells and optical-phase retardation set-up*

The cells used consisted of liquid crystalline material between two ITO covered glass plates whose inner surfaces were coated with rubbed polyimide films. The rubbing was done with the aid of a machine similar to the one described by Becker *et al.* [15]. It consisted of a velvet-coated drum rotating at a constant speed, which was transported over the polyimide layer at a constant speed. The rubbing strength was controlled via the pile impression of the velvet on the substrate [16, 17]. The two substrates were assembled with the rubbing directions either parallel or antiparallel.

A constant cell gap of 1·6 μm was maintained with the aid of quartz spacer beads. The spacer beads were applied by means of spincoating from a suspension of the spacer beads in propan-2-ol on one of the substrates.

The optical-phase retardation was measured for these liquid crystal cells as a function of the angle of incidence of a laser beam (wavelength 632·8 nm) in a set-up described in [10]. The pretilt angle can be derived from the measured data by means of a fitting procedure using a model for the liquid crystal structure. This will be discussed in § 3. For nematic liquid crystal layers and antiparallel rubbing directions, the structure is assumed to be that with the lowest deformation energy, that is the one in which the director tilt equals the surface pretilt over the entire cell thickness. In this case, the accuracy of the pretilt angle derived from the data measured in our set-up is typically within 0·1°.

The nematic material used was 4′-*n*-pentyl-4-cyanobiphenyl (5CB). The smectic A material used was S5, which is a mixture of cyanobiphenyl and cyanoterphenyl compounds. Both materials were provided by Merck Ltd. (Poole, U.K.). The phase sequences of these materials are:

5CB: C (23·5°C) N (35·5°C) I
S5: C (1°C) S_A (55·5–55·7°C) N (57·5–61°C) I.

The ordinary and extraordinary refractive indices are respectively 1·531 and 1·709 for 5CB [18], and 1·509 and 1·699 for S5 [19].

The cells were filled with the liquid crystalline material in the isotropic phase and were slowly cooled to room temperature (1°C min^{-1}). For both materials a homogeneous alignment was obtained.

2.2. *Experimental determination of the smectic layer structure*

Before it is possible to derive values for the pretilt angle from the measured optical-phase retardation data, the liquid crystal structures in our smectic cells have to be identified as tilted-bookshelf (see figure 2) or chevron-type (see figure 3) structures. To this end we performed X-ray diffraction experiments and made observations by microscopy.

The X-ray diffraction measurements were carried out using a Philips PW3020 Goniometer with a divergence slit of 0·25°, a receiving slit of 0·2 mm and an anti-scatter slit of 0·25°. A normal Cu long fine focus tube running at 45 kV and 45 mA was used. Because the X-rays hit the sample at a high angle of incidence (φ) and the diffraction angle (2θ) is low, the measurement is actually in transmission (see inset of figure 4). Due to this non-focusing geometry, the 2θ resolution is limited to 0·5°. The zero points of the φ and 2θ-axis were determined to within 0·025° by scanning φ versus 2θ with the sample parallel with the X-ray beam and optimizing the sample shadow. The substrate thickness of the cells used for X-ray measurements was 150 μm. The cell gap was 4·6 μm.

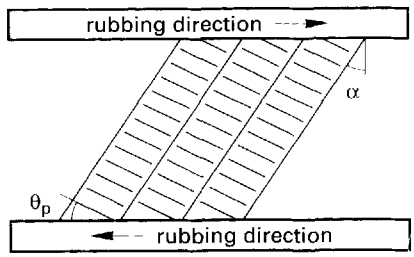

Figure 2. Smectic A liquid crystalline material with a tilted-bookshelf layer structure in a cell whose two orienting surfaces have been rubbed in antiparallel directions. The layer tilt angle α and the pretilt angle θ_p are indicated.

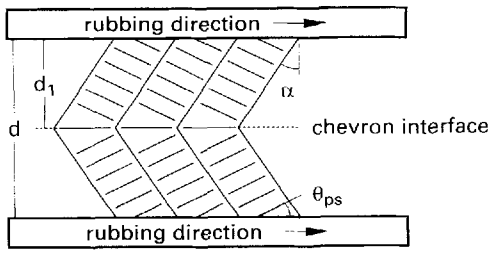

Figure 3. Smectic A liquid crystalline material with a chevron layer structure. The two orienting surfaces of the cell have been rubbed in parallel directions. Indicated are the layer tilt angle α, the surface pretilt angle θ_{ps}, the cell thickness d and the distance between the chevron interface and one substrate d_1.

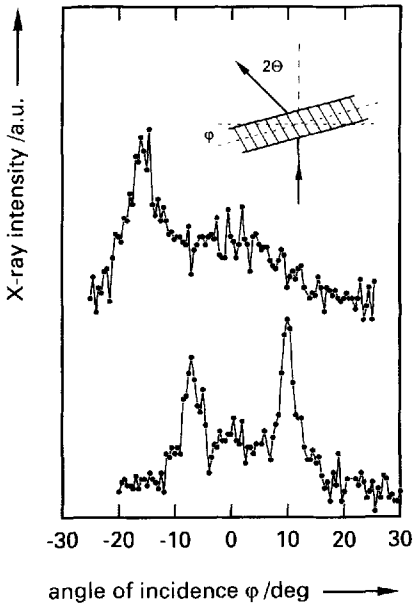

Figure 4. X-ray diffraction profiles of the smectic A liquid crystal material S5 oriented in cells for which the rubbing directions of the alignment layers were antiparallel (upper curve, tilted-bookshelf layer structure) or parallel (lower curve, chevron layer structure). The inset shows a schematic of the X-ray diffraction set-up.

The presence of the tilted-bookshelf layer structure in cells with antiparallel rubbing directions was confirmed by these measurements. The result is shown in figure 4 (upper curve). A single diffraction peak is observed at an angle of $-17°$. Microscopic observations showed a uniform appearance without defect lines.

X-ray diffraction experiments on the parallel rubbed cells showed peaks at $+10°$ and at $-7°$ (lower curve in figure 4). A small asymmetry (25 per cent) in peak heights is noticed. The occurrence of two peaks is characteristic for the chevron layer structure (see figure 3) [11, 12, 20–22]. In these cells with a chevron-type layer structure, focal–conic defects are observed. The appearance of these focal–conic defects is attributed to the relaxation of strain at the chevron interface and at the aligning surfaces [22]. The direction is determined by the chevron orientation. Zigzag defect lines mark boundaries between areas with opposite directions of the focal–conic defects. We used these cells to determine the relation between the rubbing axis and the chevron direction as inferred from the focal–conic defect orientation. A homogeneously aligned smectic A texture free of zigzag defects was obtained by the use of a polyimide alignment layer that induces a high pretilt angle ($\approx 10°$) in the case of nematics. For this orientation layer, the direction of the chevron tip is opposite to the rubbing direction.

3. Model systems and calculations

3.1. *The phase retardation method*

A nematic or a smectic A medium can be uniaxially and homogeneously aligned between two substrates rubbed in antiparallel directions (see figures 1 and 2). A light beam passing through this birefringent medium is split into an ordinary and an extraordinary beam, each propagating independently and with a different velocity. The phase retardation of the extraordinary beam with respect to the ordinary beam depends on the optical anisotropy and the direction of the optical axis of the liquid crystalline medium, the cell thickness and the angle of incidence (angle of the incident light beam with respect to the axis normal to the cell substrates). The angle between the optical axis and the aligning substrate is defined as the pretilt angle.

The direction of the optical axis can be determined by measuring the phase retardation as a function of the angle of incidence. In this so-called phase retardation method [10], which is based on the crystal rotation method [5], the angle of incidence is varied by rotating the cell around an axis which is perpendicular to the plane of incoming and outgoing beams. This plane also contains the optical axis of the liquid crystal layer. The values for the pretilt angle and the cell thickness were derived by fitting the analytical expression for the angular dependence of the phase retardation to the measured curve. Only the extraordinary refractive index and the ordinary refractive index of the liquid crystalline medium at the measuring wavelength were then required. The phase retardation method is therefore a fast and simple technique for measuring the pretilt angle with a high degree of accuracy, regardless of the pretilt angle size or the cell thickness.

3.2. *Nematic model system*

The simplest system for pretilt measurements is the nematic phase confined in a planar cell with antiparallel rubbing directions of the top and bottom substrates. A uniform direction of the optical axis throughout the cell is then obtained (see figure 1).

The phase retardation (δ) induced by this nematic medium is given by the following expression [4]:

$$\delta = \frac{2\pi}{\lambda} d\left[\frac{n_o^2 - n_e^2}{n^2} \sin\theta_p \cos\theta_p \sin\varphi + \frac{n_o n_e}{n^2}\sqrt{(n^2 - \sin^2\varphi)} - \sqrt{(n_o^2 - \sin^2\varphi)}\right], \quad (1)$$

with

$$n^2 = n_o^2 \cos^2\theta_p + n_e^2 \sin^2\theta_p, \quad (2)$$

where d denotes the liquid crystal layer thickness, φ the angle of incidence with respect to the substrate normal, θ_p the pretilt angle, λ the wavelength, n_o the ordinary and n_e

the extraordinary refractive index. The angle of incidence at which the maximum phase retardation is obtained is determined by the value and sign of the pretilt angle. The magnitude of the phase retardation is linearly dependent on the layer thickness.

The layer thickness and the pretilt angle of the liquid crystal sample can be unambiguously determined by fitting equation (1), using d and θ_p as fitting parameters [10], to the measured curve.

3.3. *Smectic A tilted-bookshelf layer model*

A few groups [8, 23, 24] have performed pretilt measurements on smectic media with the tilted-bookshelf layer structure. The tilted-bookshelf layer structure can be obtained by rubbing the two aligning surfaces in opposite but parallel directions (see figure 2). This has been observed in the case of high-pretilt polyimide layers [13], as well as in the case of obliquely evaporated SiO_x [14]. For this structure, in order to calculate the optical phase retardation, we again assume a homogeneous, tilted layer structure with a constant angle between the director and the cell surfaces throughout the cell (see figure 2). Therefore, the measured relation between the phase retardation and the angle of incidence can be described by equation (1), as in the nematic model. The pretilt angle and the cell thickness can be determined with the same accuracy as in the case of the nematic system.

3.4. *The smectic A chevron layer model*

The chevron layer structure (see figure 3) can be obtained in the smectic A phase by rubbing the two aligning surfaces in the same direction. The presence of the chevron layer structure can be shown by X-ray measurements [11, 12, 20–22] and is recognizable by focal–conic defects [22] or by zigzag defects [11]. The bending plane of the smectic layers (chevron interface or chevron tip) is parallel to the cell substrates. The symmetric chevron structure is characterized by a chevron interface in the middle of the cell. X-ray measurements can yield an indication of the degree of symmetry of the chevron layer structure [25].

In order to be able to estimate the pretilt angle in a cell rubbed in parallel directions, a model is required which takes into account the chevron layer structure. We therefore divided the liquid crystal layer into two parts of thicknesses d_1 and $d - d_1$ (see figure 3), where d is the cell thickness and d_1 the distance from the chevron tip to one of the substrates. Each part corresponds to a uniformly tilted layer structure, with opposite tilt directions and opposite pretilt angles. When the sample is inserted into the phase retardation set-up, the incident light beam passes through the liquid crystalline medium and emerges at the other side with a phase shift which is the sum of the phase retardation contributions of the two birefringent parts of the cell: $\delta = \delta_+ + \delta_-$, with

$$\delta_+ = \frac{2\pi}{\lambda} d_1 \left[\frac{n_o^2 - n_e^2}{n^2} \sin\theta_p \cos\theta_p \sin\varphi + \frac{n_o n_e}{n^2} \sqrt{(n^2 - \sin^2\varphi)} - \sqrt{(n_o^2 - \sin^2\varphi)} \right], \quad (3)$$

$$\delta_- = \frac{2\pi}{\lambda} (d - d_1) \left[-\frac{n_o^2 - n_e^2}{n^2} \sin\theta_p \cos\theta_p \sin\varphi + \frac{n_o n_e}{n^2} \sqrt{(n^2 - \sin^2\varphi)} - \sqrt{(n_o^2 - \sin^2\varphi)} \right]. \quad (4)$$

The total phase retardation δ can now be calculated and is expressed by

$$\delta = \frac{2\pi}{\lambda} d \left[(2d_{tip} - 1) \frac{n_o^2 - n_e^2}{n^2} \sin\theta_p \cos\theta_p \sin\varphi + \frac{n_o n_e}{n^2} \sqrt{(n^2 - \sin^2\varphi)} - \sqrt{(n_o^2 - \sin^2\varphi)} \right] \quad (5)$$

where $d_{tip} = d_1/d$ defines the relative chevron interface position in the liquid crystalline medium ($0 < d_{tip} < 1$).

At the chevron interface, the molecules are parallel to the cell substrate, as a result of which the pretilt angle is locally zero. At the aligning surfaces, the molecules adopt an angle θ_{ps}. The value of this surface pretilt angle θ_{ps} depends on the interaction with and the morphology of the aligning surface, as well as on the elastic interactions with the liquid crystal molecules in the bulk. The angle between the optical axis and the substrate surface therefore varies from θ_{ps} at the surface to zero degrees at the chevron interface and equation (5) must be modified to account for this.

In order to describe the splayed variation in pretilt angle across the cell, we assume the relation $\theta_p = \theta_{ps}(1 - z^\beta)$ to hold, where the exponent β is a positive number and z ranges from 0 at the aligning surface to 1 at the chevron interface. For $\beta = 1$, the variation of the pretilt angle from the surface to the chevron interface is linear. For $0 < \beta < 1$, the part of the director profile with the strongest splay deformation is near the surfaces, while for $\beta > 1$, the strongest splay is found near the chevron tip. An increase in the exponent β implies a decrease in the thickness of the chevron interface region. For β going to infinity, the thickness of the chevron interface region vanishes. In this case, the chevron structure corresponds to a constant pretilt angle on both sides of the chevron interface ($\theta_p = \theta_{ps}$) and consequently to a discontinuous transition of the pretilt angle at the chevron interface. By dividing the upper and lower parts of the chevron into N sublayers of thickness d_1/N and $(d - d_1)/N$, respectively, with each sublayer having its own pretilt angle θ_p, the phase

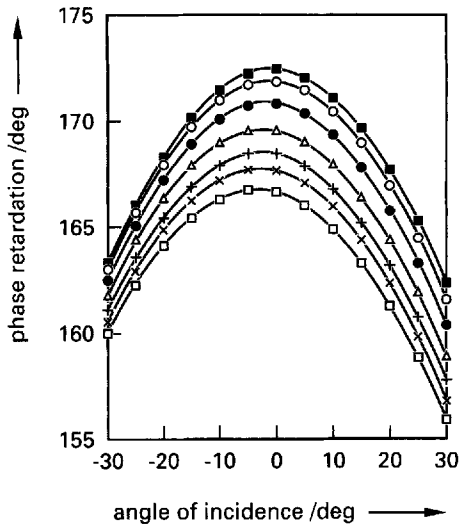

Figure 5. Results of the calculation of the phase retardation as a function of the angle of incidence for a smectic A material with an asymmetric chevron layer structure ($d_{tip} = 0{\cdot}55$). The surface pretilt angle θ_{ps} was fixed at 10°, whereas the exponent β was varied (■, $\beta = \frac{1}{4}$; ○, $\beta = \frac{1}{2}$; ●, $\beta = 1$; △, $\beta = 2$; +, $\beta = 4$; ×, $\beta = 8$; □, $\beta = \infty$). The cell thickness d was 1·6 μm and the number of sub-layers N was 100.

retardation, as a function of the surface pretilt angle θ_{ps}, is calculated to be

$$\delta = \frac{2\pi d}{\lambda N} \sum_{i=1}^{N} \left[(2d_{tip} - 1) \frac{n_o^2 - n_e^2}{n^2} \times \sin(\theta_{ps}(1 - z^{\beta})) \cos(\theta_{ps}(1 - z^{\beta})) \sin\varphi + \frac{n_o n_e}{n^2} \sqrt{(n^2 - \sin^2\varphi)} - \sqrt{(n_o^2 - \sin^2\varphi)} \right] \quad (6)$$

with

$$z = (i - 1)/N$$

and

$$n^2 = n_o^2 \cos^2(\theta_{ps}(1 - z^{\beta})) + n_e^2 \sin^2(\theta_{ps}(1 - z^{\beta})).$$

If the number of sublayers N is set to 1, we obtain the same situation as for β is infinite. In this case the phase retardation is expressed by equation (5).

Figure 5 presents the results of a computer calculation of the phase retardation as a function of the angle of incidence for different values of β in the case of an asymmetric chevron structure ($d_{tip} = 0{\cdot}55$) and a fixed surface pretilt angle ($\theta_{ps} = 10°$). The number of sublayers was taken to be so large ($N = 100$, corresponding to 200 sublayers in the entire cell gap) that a further increment of N no longer led to an observable change in the calculated curve.

As for the nematic model, the above equation for the chevron model yields a linear dependence of the phase retardation on the cell thickness. The two other parameters, θ_{ps} and d_{tip}, determine the exact position of the maximum of the $\delta(\varphi)$ curve. As is shown in figure 6 and figure 7, the phase retardation decreases with an increasing surface pretilt angle. For the asymmetric chevron structure, i.e. $d_{tip} \neq \frac{1}{2}$, a variation in pretilt angle also causes a horizontal shift of the phase-retardation curve (see figure 7). The phase-retardation measurements make it possible to distinguish between a symmetric chevron structure and an asymmetric one.

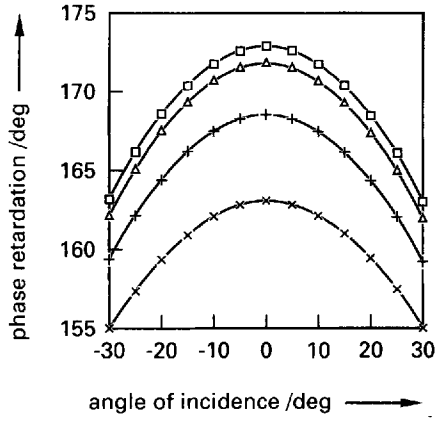

Figure 6. Calculated values of the phase retardation as a function of the angle of incidence for a smectic A material with a symmetric chevron layer structure ($d_{tip} = \frac{1}{2}$). The exponent β was fixed at 4, whereas the surface pretilt angle θ_{ps} was varied (□, $\theta_{ps} = 0°$; △, $\theta_{ps} = 5°$; +, $\theta_{ps} = 10°$; ×, $\theta_{ps} = 15°$). The cell thickness d was 1·6 μm and the number of sub-layers N was 100.

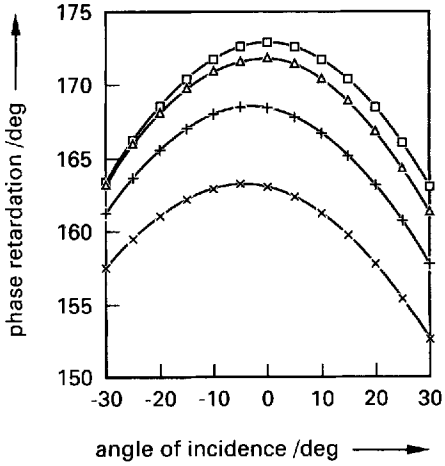

Figure 7. Calculated results for the phase retardation as a function of the angle of incidence for a smectic A material with an asymmetric chevron layer structure ($d_{tip} = 0{\cdot}55$). The exponent β was 4, whereas the surface pretilt angle θ_{ps} was varied (□, $\theta_{ps} = 0°$; △, $\theta_{ps} = 5°$; +, $\theta_{ps} = 10°$; ×, $\theta_{ps} = 15°$). The cell thickness d was 1·6 μm and the number of sub-layers N was 100.

The three unknown independent parameters (d, θ_{ps}, d_{tip}) are determined with the aid of a fitting procedure using equation (6) and assuming the exponent β to have a certain value to be specified in § 4.2.2. It turned out to be convenient to apply a hyperbolic scaling of these parameters

$$d_{tip} = \frac{d_{tip}^{max} + d_{tip}^{min} \exp(-2X_{tip})}{(1 + \exp(-2X_{tip}))}, \quad (7)$$

$$\theta_{ps} = \frac{\theta_{ps}^{max} + \theta_{ps}^{min} \exp(-2X_{\theta})}{(1 + \exp(-2X_{\theta}))}, \quad (8)$$

and

$$d = \frac{d_{max} + d_{min} \exp(-2X_{d})}{(1 + \exp(-2X_{d}))}, \quad (9)$$

in which X_{θ}, X_{tip} and X_{d} are the new fitting parameters and d_{max}, d_{min}, θ_{ps}^{max}, θ_{ps}^{min}, d_{tip}^{min} and d_{tip}^{max} depend on the sample preparation conditions. For example, equation (7) with $d_{tip}^{min} = 0$ and $d_{tip}^{max} = 1$ ensures that the chevron interface lies inside the cell.

4. Experimental results

First, we performed phase retardation measurements using empty cells without alignment layers. The average phase retardation measured for different angles of incidence was $-0{\cdot}15 \pm 0{\cdot}22°$. This low value can be attributed to the small intrinsic birefringence of the cell. It shows that the contribution of the cell substrates to the measured phase retardation is low.

4.1. *Pretilt angle measurements for the nematic phase*

In order to be able to compare the pretilt angle in the smectic A phase with that in the nematic phase, we measured the pretilt angle for 5CB using the same alignment conditions as for S5 (spacer bead diameter, alignment layer and rubbing strength).

Figure 8 presents the measured phase retardation versus the angle of incidence for 5CB at different rubbing strengths. The rubbing strength was enhanced by increasing the pile impression. The pretilt angle was determined by fitting equation (1) to the measured curve. The dependence of the pretilt angle on the pile impression is plotted in figure 11. The pretilt angle was found to increase with decreasing rubbing strength, which is in accordance with the literature [26].

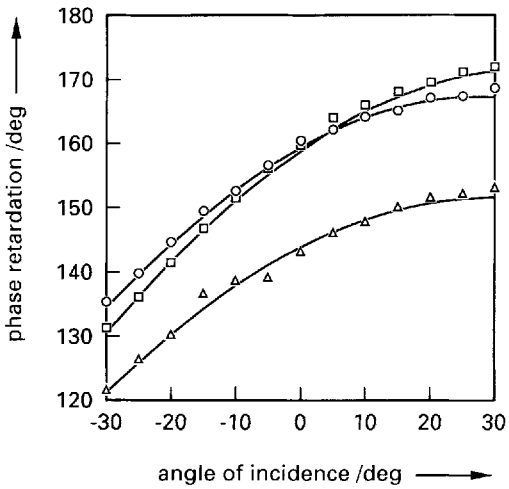

Figure 8. Results of the measurement of the phase retardation as a function of the angle of incidence for the nematic liquid crystal 5CB. The results obtained for the different pile impressions used during the rubbing are shown (□, 0·2 mm; ○, 0·3 mm; △, 0·4 mm). The solid lines are the fitted curves obtained using equation (1).

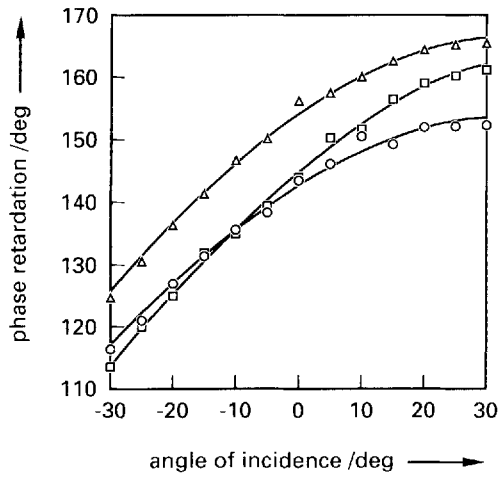

Figure 9. Results of the measurement of the phase retardation as a function of the angle of incidence for the smectic A liquid crystal S5 with a tilted-bookshelf layer structure. The results obtained for the different pile impressions used during the rubbing are shown (□, 0·2 mm; △, 0·3 mm; ○, 0·4 mm;). The solid lines are the fitted curves obtained using equation (1).

4.2. *Pretilt angle measurements in the smectic A phase*

4.2.1. *Smectic A tilted-bookshelf structure*

Figure 9 shows the measured phase retardation curves obtained for smectic A cells rubbed in antiparallel directions for different pile impressions. The pretilt angle was determined by fitting equation (1) to the measurements (nematic model) and the results are plotted in figure 11. As in the case of the nematic phase, the pretilt angle decreases with increasing rubbing strength. The pretilt angle determined for the tilted-bookshelf layer structure was found to be higher than in the case of the nematic phase.

4.2.2. *Smectic A chevron layer structure*

The measurements performed on smectic A cells with parallel rubbing directions show a dependence of the phase

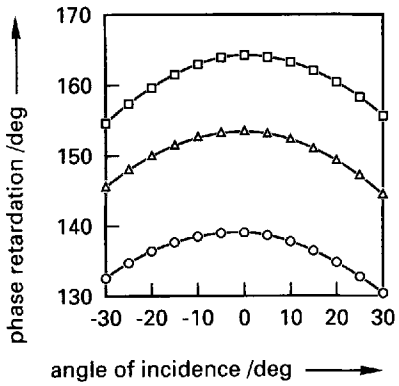

Figure 10. Results of the measurement of the phase retardation as a function of the angle of incidence for the smectic A liquid crystal S5 with a chevron layer structure. The results obtained for the different pile impressions used during the rubbing are shown (○, 0·2 mm; △, 0·3 mm; □, 0·4 mm;). The solid lines are the fitted curves obtained using equation (6), with $\beta = 4$ and $N = 100$.

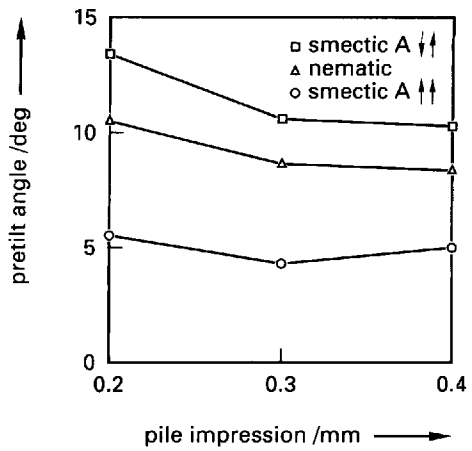

Figure 11. Pretilt angles determined from the phase retardation measurements as a function of the pile impression for the nematic liquid crystal 5CB (△) and the smectic A material S5 with a tilted-bookshelf layer structure (□) and a chevron layer structure (○).

retardation on the angle of incidence that differs from the dependence for cells with antiparallel rubbing directions. The curves measured for different pile impressions of the rubbing cloth used are presented in figure 10. The shape of the measured curves is characteristic of the chevron layer structure and is in agreement with the results of the calculations (see § 3.4). All the curves show a small degree of asymmetry which is independent of the pile impression.

As follows from § 3.4, the surface pretilt angle obtained from the phase retardation measurements depends on the value of the exponent β used. Model calculations showed that for small pretilt values and a small chevron asymmetry, a change from $\beta = 4$ to $\beta = \frac{1}{4}$ has a small effect on the calculated curves for the phase retardation as a function of the angle of incidence. For $d_{tip} = 0{\cdot}55$ and $\theta_{ps} = 5°$, the calculated phase retardation for these two β values differed by at most 0·6° over the range of incidence angles considered here. A value of $\beta < 1$ would mean a relatively thick central part with small tilt values. The corresponding X-ray diffraction peak (see figure 4, lower curve) in this tilt angle range was observed to be small. Therefore we chose to do our analysis with director profiles with $\beta > 1$. So in our model, the region with the strongest splay deformation is near the chevron tip. Values for the exponent β ranging from 4 to infinity would only slightly influence the deduced value of the surface pretilt angle (by less than 2°). The magnitude of β was taken to be 4. However, it must be noted that our measurement technique is not particularly suited to infer conclusions on the variation of the director orientation across the cell's thickness, as the measured phase retardation is a sum of the contributions of the sub-layers in the cell, irrespective of the order in which these sublayers are stacked.

The surface pretilt angles (θ_{ps}) determined via a fit to the experimental data are presented in figure 11. The results show that the surface pretilt angle is less dependent on the rubbing strength than in the case of the nematic or the tilted-bookshelf smectic A phase. Furthermore, the surface pretilt angle was found to be smaller than the pretilt angles obtained for the nematic and the tilted-bookshelf A phases. This last result agrees with the results recently obtained by Elston [27].

In the fitting, the position of the chevron interface d_{tip} was found to lie away from the middle of the cell. A value of d_{tip} of $0{\cdot}55 \pm 0{\cdot}03$ was obtained. The position of the chevron interface was found to be independent of the rubbing strength.

5. Discussion

We have measured the pretilt angle in the smectic A phase and have compared the results with similar measurements on identical cells filled with a nematic liquid crystal. Differences were found. In the first part of this section, the results for the tilted bookshelf smectic A cells are compared to those of nematic cells. In the second part, the differences between the two types of smectic A cells will be discussed: The tilted-bookshelf and the chevron-type cells.

The occurrence of the tilted-bookshelf layer structure in antiparallel rubbed smectic A cells was proven by X-ray diffraction (see figure 4). The phase-retardation curves obtained for this smectic A tilted-bookshelf layer structure can be analysed using the same model as that used for the nematic phase. It was found that the pretilt angle in the smectic A tilted-bookshelf structure was higher than that obtained for the nematic phase. The pretilt angle therefore seems to depend on the liquid crystalline phase. It needs to be considered that the chemical composition of the

smectic A (S5) and of the nematic material (5CB) was different. Whereas 5CB consists of cyanobiphenyl mesogenic units, the smectic A material is a mixture of cyanobiphenyl and cyanoterphenyl compounds. This difference in chemical composition may have caused a small difference in pretilt angle, but we think that this is insufficient to explain the large difference measured.

The pretilt angle determined from the optical-phase retardation measurements differs from the angle at which the X-ray diffraction peak in the upper curve of figure 4 appears. This may be explained by the observation that the direction of the optical axis, that is measured in the phase retardation experiment, differs from the direction of the mechanical axis that is probed in the X-ray diffraction measurements. The difference between these directions (i.e. the principal axis of the optical tensor and the axis of the least moment of inertia) depends on the conformation of the alkyl chain in the molecules and its absolute value is expected to be in the range of 0–10° [28]. From our measurements we derive a difference of $-4°$.

The results of the phase retardation measurements on the smectic A chevron structure, as indicated by two X-ray diffraction peaks (see figure 4), have to be analysed using a model that makes allowance for the change in pretilt angle between the aligning surface and the chevron interface. The significant difference between the pretilt angles measured in the chevron layer structure (5°) and those in the tilted-bookshelf structure (13°) indicates a dependence of the pretilt angle on the liquid crystal layer structure. With respect to the dependence of the pretilt angle on the rubbing strength, we conclude that the pretilt is primarily determined by bulk properties of the liquid crystal layer (thermal shrinkage of smectic layer thickness). This agrees with literature results [29] that indicate only a small influence of the orientation layer material on smectic layer tilt angles, as measured with X-ray diffraction. Again, we find a difference between the surface pretilt angle (lower curve in figure 11) and the position of the X-ray diffraction peaks. The sign and magnitude of this difference agrees with the corresponding difference found for the tilted-bookshelf cells.

The director in the smectic A phase is preferentially aligned parallel to the layer normal. Therefore the chevron structure is highly strained at the chevron interface. A transition region will exist at the aligning surface, in which the tilt of the molecules varies from the surface pretilt value to zero at the chevron interface. The surface value will depend on the bulk elastic constants and on the anchoring energy of the molecules to the surface. In the case of weak anchoring, the chevron structure will alter the surface pretilt angle. As follows from the results of our experiments, this means that the surface pretilt angle is smaller in the chevron layer structure than that in the tilted-bookshelf layer structure or that in the nematic phase. This observation is in agreement with the results recently published by Elston [27], who measured the surface pretilt angle in splayed nematic and smectic A materials with substrates inducing high-pretilt angles using optical-mode techniques. The transition region, in which the pretilt angle varies from the surface value to the bulk value, was determined to be 0·5 μm thick [27]. In our model, presented in § 3.4, we used $\beta = 4$, and in that case the pretilt angle decreases to 90 per cent of its surface value in approximately 0·5 μm.

A small degree of asymmetry was observed in the optical-phase retardation measurements and in the X-ray diffractogram of the chevron-type cells. This is indicative of an asymmetric director profile in the cell; it may have been caused by an asymmetry in the cell-production process, for example in the spin coating of the spacer beads from a propan-2-ol suspension on to one of the substrates. In our fitting model, the asymmetry in the phase retardation curves is interpreted as a shift of the chevron interface a short distance away from the centre of the cell ($d_{tip} = 0{\cdot}55$). This agrees with the observed difference in heights of the X-ray diffraction peaks. However, another possibility would be to allow for different pretilt angles at the aligning surfaces. This too would be in accordance with the X-ray measurements. We tested this in model calculations. It turned out to be possible to generate a similar asymmetry in the curves by varying the surface pretilt angles and keeping the chevron interface at the centre of the cell. The effect of a shift of the chevron interface of 10 per cent, which is the degree of asymmetry that was derived from our measurement data, would correspond to 25 per cent variation in the surface pretilt angles in the case of a chevron with its interface fixed at the centre of the cell. Yet another possibility, of course, is to allow variations in both the surface pretilt angles and the chevron tip position. In that case, the fitting procedure would involve four fitting parameters. We tried to fit our data with those parameters, but it turned out to be impossible to arrive at conclusive values for these parameters from our measurement results. Apparently, the type of curves that we have measured is not suitable for a four-parameter fitting procedure. We chose to use equal surface pretilt values for both chevron segments and used the chevron interface position to account for the asymmetry in the cell.

One way of studying the effect of the chevron structure on the surface pretilt in more detail is by varying the temperature. As the chevron angle (α) is temperature-dependent, pretilt angle measurements at elevated temperatures will demonstrate more clearly the influence of the chevron structure. Pretilt angle measurements in the nematic phase of S5 could give more information on the effect of the liquid crystalline phase on the pretilt angle. We performed these measurements, but the lack of data on

the refractive indices at higher temperatures prohibited interpretation of the results.

6. Conclusions

As shown by the results of measurements using the phase retardation method, the pretilt angle in the smectic A phase depends on the layer structure. The pretilt angle was found to be smaller in the case of the chevron layer structure than in the case of the tilted-bookshelf layer structure.

An effect of the liquid crystal phase was also observed. The pretilt angle appeared to be smaller in the nematic phase than in the tilted-bookshelf smectic A phase. Care should be taken in deducing pretilt angles for smectic materials from the results of measurements performed using nematic liquid crystals.

We are grateful to C. J. Gerritsma for helpful discussions and suggestions. We also wish to thank G. T. Jaarsma for his help in computing, A. H. Bergman for improvements of the measuring set-up and G. G. H. van de Spijker and W. A. M. Brankaert for their support in preparing the cells.

References

[1] MOTOOKA, T., FUKUHARA, A., and SUZUKI, K., 1979, *Appl. Phys. Lett.*, **34,** 305.

[2] STIEB, A. VON, BAUR, G., and MEIER, G., 1974, *Ber. Bunsenges.*, **78,** 899.

[3] YAMAMOTO, N., YAMADA, Y., MORI, K., ORIHARA, H., and ISHIBASHI, Y., 1989, *Jap. J. appl. Phys.*, **28,** 524.

[4] SCHEFFER, T. J., and NEHRING, J., 1984, *Appl. Phys. Lett.*, **45,** 1021.

[5] BAUR, G., WITTWER, V., and BERREMAN, D. W., 1976, *Phys. Lett.*, **56,** 142.

[6] SCHEFFER, T. J., and NEHRING, J., 1977, *J. appl. Phys.*, **48,** 1783.

[7] See, for example: NEGI, Y. S., SUZUKI, Y., HAGIWARA, T., KAWAMURA, I., YAMAMOTO, N., MORI, K., YAMADA, Y., KAKIMOTO, M., and IMAI, Y., 1993, *Liq. Crystals*, **13,** 153; ITOH, N., KODEN, M., MIYOSHI, S., and WADA, T., 1993, *Liq. Crystals*, **15,** 669; OKADA, H., NINOMIYA, N., MURASHIRO, K., ONNAGAWA, H., and MIYASHITA, K., 1993, *J. SID*, **1,** 277.

[8] HAUCK, G., and KOSWIG, H. D., 1990, *Molec. Crystals liq. Crystals*, **179,** 435.

[9] A general review on this subject is given by JÉRÔME, B., 1991, *Rep. Prog. Phys.*, **54,** 391.

[10] VAN SPRANG, H. A., 1991, *Molec. Crystals liq. Crystals*, **199,** 19.

[11] RIEKER, T. P., CLARK, N. A., SMITH, G. S., PARMAR, D. S., SIROTA, E. B., and SAFINYA, C. R., 1987, *Phys. Rev. Lett.*, **59,** 2658; RIEKER, T. P., CLARK, N. A., SMITH, G. S., and SAFINYA, C. R., 1989, *Liq. Crystals*, **6,** 565.

[12] TAKANISHI, Y., OUCHI, Y., TAKEZOE, H., and FUKUDA, A., 1989, *Jap. J. appl. Phys.*, **28,** L487.

[13] ORIHARA, H., SUZUKI, A., ISYHIBASHI, Y., GOUHARA, K., YAMADA, Y., and YAMAMOTO, N., 1989, *Jap. J. appl. Phys.*, **28,** L676.

[14] OUCHI, Y., LEE, J., TAKEZOE, H., FUKUDA, A., KONDO, K., KITAMURA, T., and MUKOH, A., 1988, *Jap. J. appl. Phys.*, **27,** L1993.

[15] BECKER, M. E., KILIAN, R. A., KOSMOWSKI, B. B., and MLYNSKI, D. A., 1986, *Molec. Crystals liq. Crystals*, **132,** 167.

[16] VAN AERLE, N. A. J. M., BARMENTLO, M., and HOLLERING, R. W. J., 1993, *J. appl. Phys.*, **74,** 3111.

[17] UCHIDA, T., HIRANO, M., and SAKAI, H., 1989, *Liq. Crystals*, **5,** 1127.

[18] WU, S. T., WU, C. S., WARENGHEM, M., and ISMAILI, M., 1993, *Opt. Engng*, **32,** 1775.

[19] Data provided by Merck Ltd (Poole, U.K.).

[20] CLARK, N. A., and RIEKER, T. P., 1988, *Phys. Rev.* A, **37,** 1053.

[21] OUCHI, Y., TKANO, H., TAKEZOE, H., and FUKUDA, A., 1988, *Jap. J. appl. Phys.*, **27,** 1.

[22] OUCHI, Y., TAKANISHI, Y., TAKEZOE, H., and FUKUDA, A., 1989, *Jap. J. appl. Phys.*, **28,** 2547.

[23] YANG, K. H., LIEN, A., and CHIEU, T. C., 1988, *Jap. J. appl. Phys.*, **27,** 2022.

[24] TSUBOYAMA, A., HANYU, Y., YOSHIHARA, S., and KANBE, J., 1992, *Proceedings of the 12th International Display Research Conference (Japan Display '92)*, p. 53.

[25] KONDO, S., and AKAHANE, T., 1991, *Jap. J. appl. Phys.*, **30,** L1659.

[26] KUNIYASU, S., FUKURO, H., MAEDA, S., NAKAYA, K., NITTA, M., OZAKI, N., and KOBAYASHI, S., 1988, *Jap. J. appl. Phys.*, **27,** 827.

[27] ELSTON, S. J., 1994, *Liq. Crystals*, **16,** 151.

[28] MYRVOLD, B. E., KONDO, K., and OH-HARA, S., 1994, *Molec. Crystals liq. Crystals*, **239,** 211.

[29] OUCHI, Y., LEE, J., TAKEZOE, H., FUKUDA, A., KONDO, K., KATIMURA, T., and MUKOH, A., 1988, *Jap. J. appl. Phys.*, **27,** L725; ITOH, N., NARUTAKI, Y., SHINOMIYA, T., KODEN, M., MIYOSHI, S., and WADA, T., 1992, *Jap. J. appl. Phys.*, **31,** 1414.